



Localized correlation treatment using natural bond orbitals

N. Flocke, Rodney J. Bartlett *

Department of Chemistry and Physics, Quantum Theory Project, University of Florida, Gainesville, FL 32611, USA

Received 8 July 2002; in final form 4 October 2002

Abstract

We present studies using natural bond orbitals (NBOs) as a starting point for a localized electron correlation treatment, as these kind of localized orbitals lead to CCSD results which show significant transferability and exponential decay patterns in the T_2 amplitudes. The NBO CCSD approach combines the advantages of both the HF CCSD formulation (less amplitudes, orthogonal orbitals) and the AO-based CCSD strategy (fast decay of amplitudes and integrals).

© 2002 Elsevier Science B.V. All rights reserved.

1. Introduction

Traditional correlated methods use HF MOs which are highly delocalized over the entire molecular system. This property leads to exponential scaling behavior in computer time with an increasing number of electrons. In the HF MO description, electron correlation can become unphysical in the sense that it appears to be smeared over the entire molecular system, rather than being properly ‘short-sighted’, to use the term of W. Kohn. While the idea of using localized orbitals in electron correlation treatments is as old as the field [1,2], only recently have realistic methods been developed and implemented [3–6]. The prime benefits of localized electron correlation treatments over the traditional delocalized HF

MO one only become apparent when the molecular system has a reasonably large extension in space.

Localized correlation treatments depend upon achieving sparsity in integrals, densities, or other aspects of the calculation. The oldest exploits the HF MOs themselves, which are localized by applying unitary transformations to the occupied and virtual MO sets separately. Several techniques are available for constructing these two sets of occupied and virtual localized molecular orbitals (LMOs) [7–9]. Experience with these localization procedures has shown that although it is easy to generate occupied LMOs, the virtual space is hard to localize in a satisfactory manner. The virtual orbitals constitute the residual space of a HF calculation and as such do not take part in the electron density description of the corresponding HF state, so there is no reason for the virtual space to possess any strong local character, making the results dependent on the local quality of the virtual LMOs.

* Corresponding author. Fax: +352-392-8722.

E-mail address: bartlett@qtp.ufl.edu (R.J. Bartlett).

A better approach is based on the observation that the ultimate basis in which quantum chemical calculations are being done is the AO basis, centered on the atoms in the molecule, which, once selected for a particular problem, constitutes the most local basis possible. Hence the correlation equations can be reformulated in the AO basis, at the cost of non-orthogonality, and locality is ensured by the rapid decay of the AO integrals and correlation excitation parameters with distances between atomic centers [5]. The reference function is implicitly incorporated into the AO correlation equations via the occupied and virtual space projectors of the HF one-particle reduced density matrix. The AO based formulations of electron correlation methods have the advantage of being independent of any particular MO localization procedure. However, the AO based technique, by virtue of its implicit MO \rightarrow AO reformulation of the correlation equations, must deal with the full set of AO excitation parameters ($\sim n^4$ rather than $\sim n_{\text{occ}}^2 n_{\text{virt}}^2$ in the MO approach, with n being the number of basis functions) as an additional complexity.

A third route is an LMO/AO hybrid [10]. This alleviates the difficulties experienced with proper localization of the virtual LMOs in the all LMO based correlation scheme, as the LMO picture is retained for the occupied space, but the virtual space is reformulated in terms of projected AOs obtained from the original AO basis by applying the virtual space projector. The projected AOs are orthogonal to the occupied space LMOs but non-orthogonal among themselves. Their number is the same as in the original AO basis (leading to $\sim n_{\text{occ}}^2 n^2$ excitation parameters), but, due to elimination of the required linear dependencies plus a *selection* of projected AOs for excitations according to being close in space to the occupied LMOs, their sparseness is ensured. In essence the hybrid LMO/AO approach leads to correlation equations which are intermediate in complexity between the pure MO and AO based schemes. All three mentioned localized correlation schemes are implicitly based on the HF reference function.

In this Letter, we investigate the possibility of a fourth kind of localization scheme, that was ac-

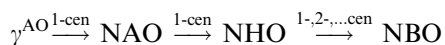
tually suggested long ago [11–13]. It retains the simplicity of the correlation equations for the all MO approach but avoids the difficulties associated with the virtual LMO space. It is also conceptually closer to how chemists think about bonds. Since in the all LMO scheme the separate localization of the occupied and virtual spaces proved to be problematic for the latter, we will relax the constraint of localizing these spaces separately, thus giving more freedom during the localization process, where more localization in the virtual space is achieved at the cost of removing some from the occupied space. This procedure will change the correlation energy as compared to the use of the HF reference function, since the associated unitary transformation corresponding to the localization procedure will mix the occupied and virtual spaces. However, results of the early investigation [11–13] showed the enormous power of CCSD for nearly any reference, since the CCSD results are virtually superimposable upon the HF based ones. In looking for an optimum occupied-virtual localization transformation we would also like to preserve the idea of a reference function, which consists of a final set of occupied and virtual localized MOs that should be a good zeroth-order approximation for application of correlation treatments. Another property we require is that we obtain potential energy curves and forces which are close to their HF counterparts. Finally, if we can achieve transferability of CC amplitudes, we open new pathways to CC solutions for very large systems.

One such possible set of localized MOs are given by the natural bond orbitals (NBOs), which were developed originally to study hybridization and covalency properties of polyatomic wavefunctions and hence were constructed to allow for interpretation of chemical phenomena in terms of the language of chemists (transition state structures and bond breaking during reactions for example). As such the NBOs represent the molecular system in a chemically intuitive way, conforming with the picture of local structures chemists assign to the distribution of electrons in molecules [14]. NBOs are obtained through a series of block-diagonalizations of the one-electron density matrix (correlated or not) and can

be grouped into five sets of orbitals: core, lone-pairs, bonds, antibonds and Rydbergs. The NBOs are orthogonal, highly localized in space, transferable from one similar molecular structure to the next and divide themselves naturally into an occupied set (core, lone-pairs and bonds) and a virtual set (antibonds and Rydbergs). The idea of using NBOs for correlation treatments has been used in connection with CASSCF calculations on some small molecular systems mainly to classify the importance of several types of NBO correlations on molecular properties [16]. However, to our knowledge, the use of NBOs as a general means to construct localized correlation methods capable of extension to large systems while avoiding exponential scaling has not been considered. Nor have they been used as a basis for CC methods.

2. Theory

In this section we briefly review the construction of the NBO basis, whose details can be found elsewhere in the literature [14,15] and at the following website: <http://www.chem.wisc.edu/~nbo5>. The starting point of the NBO procedure is the atomic m -averaged l -subblock diagonalization (l, m = atomic angular momentum shell and associated magnetic quantum numbers) of the molecular uncorrelated or correlated one-electron reduced AO density matrix γ^{AO} followed by a sequence of occupancy-weighted symmetric orthogonalizations to give the orthonormal natural atomic orbitals (NAOs) [17], classified into core, valence and Rydberg NAOs according to their density matrix occupation numbers. Next follows the construction of the atomic natural hybrid orbitals (NHOs) [18] from the valence NAOs, which are then further combined into one-, two- or more center NBOs. Below is a rough scheme for this procedure together with a table showing the type of NAOs, NHOs and NBOs and their density matrix occupation numbers one would obtain for a closed shell SCF calculation.



NAO		NHO		NBO	
Type	Occ #	Type	Occ #	Type	Occ #
Core	≈ 2	Core	≈ 2	Core	≈ 2
Va- lence	0.1– 1.9	Lone- pair Rest	≈ 2 0.1– 1.9	Lone- pair Bond Anti- bond	≈ 2 ≈ 2 ≈ 0
Ryd- berg	≈ 0	Ryd- berg	≈ 0	Ryd- berg	≈ 0

Note that although the NAOs and NHOs are more local than the final NBOs, they cannot serve the purpose of constructing a proper reference function due to their valence sets having occupation numbers that depart significantly from 2, resulting in non-quasidiagonal density matrices. On the other hand, looking at the NBO occupation numbers, we see that the density matrix in the NBO basis will be almost diagonal, i.e., its offdiagonal elements will be small. This follows readily from the essential idempotency of the SCF density matrix $\gamma \cdot \gamma = 2\gamma$, which, when taking the trace on both sides, puts an upper bound on the sum of the off-diagonal elements depending on deviations of the diagonal elements from their ideal values of 2 and 0

$$\sum_k 2\gamma_{kk} - \gamma_{kk}^2 = \sum_{k \neq \ell} \gamma_{k\ell}^2 \quad (1)$$

This property of the NBO density matrix suggests constructing a reference function in NBO space by simply filling the core, lone-pair and bond NBOs (termed Lewis NBOs in NBO theory) with two electrons each, leaving the antibond and Rydberg (non-Lewis) NBOs empty. The density matrix corresponding to such a reference function would then be strictly diagonal in the NBO space, but the Fock matrix will show non-zero elements between occupied and virtual NBOs. Note that this NBO reference function corresponds exactly to the way chemists think about the structure of molecular compounds. It is thus of high interpretative value, at the small price of only reproducing the exact HF density to a good approximation.

Choosing the NBO reference function as a starting point for correlation treatments, the resulting correlation correction will have to regain the difference in energy. In this context we state Thouless theorem [19] as follows:

Given two sets of M orthonormal spinorbitals χ and χ' related by a transformation $\chi' = \chi\mathbf{C}$, any two N -electron ($N \leq M$) determinants $|\phi\rangle$ and $|\phi'\rangle$ built from these sets are related via:

$$\frac{1}{\det(\overline{\mathbf{C}})}|\phi'\rangle = e^{\hat{T}_1}|\phi\rangle, \quad (2)$$

where \hat{T}_1 is the monoexcitation operator for $|\phi\rangle$

$$\hat{T}_1 = \sum_{ai} t_i^a a^\dagger i, \quad t_i^a = \sum_k C_{ak} \overline{C}_{ki}^{-1} \quad (3)$$

and $\overline{\mathbf{C}}$ denotes the $N \times N$ subblock of \mathbf{C} with rows and columns labeled by those spinorbitals used to build up respectively $|\phi\rangle$ and $|\phi'\rangle$.

Note that this theorem allows us to access the (unnormalized) HF determinant from the NBO determinant by a suitable set of CC \hat{T}_1 amplitudes and given these two determinants, we can always calculate the relevant \hat{T}_1 amplitudes in a straight forward manner via Eq. (3). On the contrary there is no such connection between the two determinants using CI type monoexcitation parameters (that is a linear $1 + \hat{T}_1$ instead of an exponential $e^{\hat{T}_1}$ relationship in Eq. (2)), hence the use of CC theory with inclusion of single excitations is mandatory if NBOs are to be used as a one-electron basis. The simplest sensible correlation method is thus CCSD and it is expected that the correction of the reference state is essentially due to the \hat{T}_1 amplitudes. That is, if we decompose the NBO \hat{T}_1 amplitudes into a HF correction part \hat{T}_1^0 (obtained from Eq. (3)) and a residual part \hat{T}_1^{Rest}

$$\hat{T}_1 = \hat{T}_1^0 + \hat{T}_1^{\text{Rest}}, \quad (4)$$

then we expect \hat{T}_1^{Rest} to be small in the final NBO CCSD wavefunction and comparable to the \hat{T}_1 amplitudes obtained from the corresponding HF CCSD calculation. Another way of stating this is that we expect that the \hat{T}_2 amplitudes in an NBO CCSD calculation will essentially reflect correlation between electrons in different NBOs and will

not be affected by the correction mechanism of the reference state.

For our present investigation on the use of NBO in CC methods we use the spin-independent closed shell CCSD formulation [20], implemented in standard matrix form into the QCPCACK package [21] written by one of us (N.F.). The spin-independent cluster excitation operators \hat{T}_1 and \hat{T}_2 are formulated in terms of the total spin preserving unitary group generators $E_{pq} = p_\alpha^\dagger q_\alpha + p_\beta^\dagger q_\beta$:

$$\hat{T}_1 = \sum_{ia} t_i^a E_{ai}, \quad (5)$$

$$\hat{T}_2 = \frac{1}{2} \sum_{ijab} t_{ij}^{ab} E_{ai} E_{bj}, \quad (6)$$

where indices i, j label occupied and a, b virtual orbitals. The projected CCSD equations for the correlation energy ΔE and the amplitudes are obtained by left projecting the modified Schrödinger equation $e^{-\hat{T}} H e^{\hat{T}} |0\rangle = E |0\rangle$ onto the reference function $|0\rangle$ and the complete manifold of singly and doubly excited determinants generated from $|0\rangle$. The CC correlation energy is

$$\Delta E = 2f_i^a t_i^a + w_{ij}^{ab} \left(t_{ij}^{ab} + t_i^a t_j^b \right), \quad (7)$$

where summation over all repeated indices is assumed and antisymmetrized integrals $w_{ij}^{ab} = 2\langle ab|ij\rangle - \langle ba|ij\rangle$ in Dirac notation have been used. The f_i^a denote elements of the occupied-virtual block of the Fock matrix and, as mentioned before, are non-zero in the NBO case.

3. Results

3.1. Comparison between the HF and NBO CCSD \hat{T}_1 amplitudes

Table 1 shows CCSD results obtained in comparison of the HF and NBO \hat{T}_1 amplitudes on some molecular systems at experimental geometries using the DZP basis set [22].

In this table we tabulated \hat{T}_1 amplitude vector lengths $|\mathbf{T}_1|$ of \hat{T}_1^{Rest} amplitudes for the NBO case and \hat{T}_1 amplitudes for the HF case together with the maximum absolute amplitude value $|t_1^{\text{max}}|$

Table 1

\hat{T}_1 amplitude vector lengths $|\mathbf{T}_1|$, maximum absolute \hat{T}_1 amplitude value $|t_1^{\max}|$, difference ΔE_1 between HF and \hat{T}_1^0 -projected NBO energies and CCSD/CISD energies for both HF and NBO cases for some molecular systems at experimental geometries using the DZP basis set

System	$ \mathbf{T}_1 \times 10^{-2}$		$ t_1^{\max} \times 10^{-2}$		ΔE_1	E_{CCSD}		E_{CISD}	
	HF	NBO	HF	NBO		HF	NBO	HF	NBO
CO	6.190	6.932	3.502	4.386	-0.0087	-113.0710	-113.0706	-113.0506	-113.0257
H ₂ O	2.098	2.464	1.224	1.325	-0.0023	-76.2642	-76.2645	-76.2553	-76.2505
CH ₄	1.462	1.541	0.453	0.479	0.0000	-40.4061	-40.4060	-40.3972	-40.3942
CH ₃ OH	3.190	4.189	1.098	1.705	-0.0040	-115.4551	-115.4562	-115.4239	-115.3951
C ₂ H ₄	3.649	3.753	3.108	2.370	-0.0002	-78.3808	-78.3803	-78.3532	-78.3279
C ₂ H ₆	2.060	2.095	0.645	0.491	0.0000	-79.6143	-79.6141	-79.5827	-79.5580
CH ₃ Cl	2.871	3.668	1.351	2.012	-0.0022	-499.4899	-499.4900	-499.4566	-499.4347
cyc-C ₃ H ₆	2.493	2.356	0.914	0.393	+0.0015	-117.5862	-117.5857	-117.5285	-117.4906

All energies are in a.u.

encountered in both cases and the differences $\Delta E_1 = E_0 - E_{\hat{T}_1\text{-proj}}$ between the HF energies E_0 and the \hat{T}_1^0 -projected NBO energies $E_{\hat{T}_1\text{-proj}}$. The latter were obtained by inserting the \hat{T}_1^0 amplitudes into Eq. (7) and setting all \hat{T}_2 amplitudes t_{ij}^{ab} equal to zero. As is clearly seen, the NBO CCSD \hat{T}_1^{Rest} amplitudes are comparable in magnitude with the HF CCSD \hat{T}_1 amplitudes, the corresponding vector lengths being almost equal. The projected NBO energies are also very close to the HF energies. We also present in Table 1 the HF and NBO CCSD/CISD energies for the same systems.

As expected [11–13], the corresponding CCSD energies differ only by few tens of milliHartrees. Furthermore, this result is not only true around the equilibrium geometries, as for example the PE curve for the carbon–carbon stretch in Fig. 1 shows for the ethane molecule in its staggered conformation. The HF and NBO CCSD PE curves are nearly indistinguishable with the same energy minimum around $r_{\text{CC}} = 1.54 \text{ \AA}$.

The CISD energies on the other hand, in addition to being plagued by the size-inextensivity problem, still show significant differences (in the order of $\times 10^{-2}$ Hartrees), being considerably higher than their HF counterparts, which shows clearly the inability of the single and double CI excitation parameters to correct for the use of the NBO reference function. This problem has also a severe influence on the actual computational CISD iteration process, which for the NBO case requires many more iterations (between 3 and 5 times as much for the same target accuracy) as for the HF

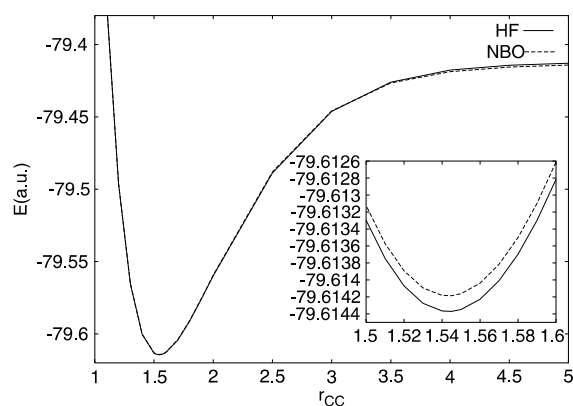


Fig. 1. PE curve for carbon–carbon dissociation of staggered C₂H₆ with geometry parameters: $r_{\text{CH}} = 1.09 \text{ \AA}$, all angles = 109.47° . Basis set used was DZP.

case. The NBO and HF CCSD calculations on the other hand have similar iteration counts, if one uses the predetermined \hat{T}_1^0 amplitudes according to Eq. (3) as a starting guess. This suggests also the possibility of performing NBO CCD calculations, in which fixed \hat{T}_1^0 amplitudes are used throughout the coupled cluster iterations. The NBO CCD approach was not examined, but would lead to similar errors as those between a HF CCD and HF CCSD calculation.

3.2. Properties of the NBO CCSD \hat{T}_2 amplitudes

We now investigate the CCSD \hat{T}_2 amplitudes, which are far more numerous than the \hat{T}_1 amplitudes (their numbers are $\text{ov}(\text{ov} + 1)/2$ and ov re-

spectively, where o and v are the number of occupied and virtual orbitals). The \hat{T}_2 amplitudes contain the pairwise correlation of electrons and, due to the two-electron nature of the molecular Hamiltonian, they constitute the most important contribution to the total electronic correlation. The NBO reference picture is particularly useful in predicting the importance of several classes of \hat{T}_2 amplitudes without actually performing a calculation. We have six kinds of electronic NBO excitations: core to antibonds, core to Rydbergs, lone-pair to antibonds, lone-pair to Rydbergs, bonds to antibonds and bonds to Rydbergs. Since electron correlation is most important between localized orbitals which are spatially close, we immediately conclude that pairwise excitations from NBO bonds to the corresponding antibonds on the same centers will be most important, i.e., will have the largest \hat{T}_2 amplitude values. The bond/antibond NBO pairs both involve the same hybrid NHOs and hence cover the same spatial region in space. Indeed, CASSCF calculations performed on the formaldehyde molecule showed that bond/antibond NBO excitations make up most of the correlation energy contribution [16]. On the other hand we expect core to Rydberg excitations on the same atomic center to be of much less importance, since these NBOs overlap much less in space. In between are the other excitation types, and due to the localized nature of the NBOs, we expect all excitations to decrease rapidly in importance as the corresponding NBO centers move apart in space. Note also that the NBO picture offers the possibility for predicting when connected triple \hat{T}_3 or higher excitations are expected to become important for a molecular correlation treatment. If more than a single bond/antibond NBO pair can be determined between the same centers, then higher than simultaneous two-fold excitations from the occupied bonds are confined near the same region in space, leading to substantial simultaneous correlation in that part of the molecular system. This is the case for molecules for which chemists intuitively write multiple bonds between atoms. For the systems studied in this Letter, all, with the exception of carbon monoxide, gave single σ -type bond/antibond pairs between two centers and all bond/antibond pairs

were found to be only localized on two centers when choosing NBO occupancy numbers >1.90 as NBO bond/antibond formation criteria.

In connection with localized correlation methods, the essential issues regarding the use of NBOs as a basis are (1) transferability of obtained excitation parameters, and (2) their magnitude falloff with separation of NBO centers involved. Transferability of the NBOs itself via evaluation of an overlap error function was studied on a series of F- and NH_2 -substituted saturated hydrocarbons [23] and was compared to the transferability of LMOs obtained for the same molecules via the Edminston–Ruedenberg procedure [8]. The conclusion drawn from that study was that transferability of the NBOs and LMOs is similar when the perturbing chemical substitution occurred directly at an NBO or LMO center, but NBOs become far more transferable compared to LMOs when the substitution was more remote. In our case we also choose a set of unsubstituted and substituted saturated hydrocarbons to examine behavior of NBO CCSD excitation parameters. As the final \hat{T}_1 amplitudes of a NBO CCSD calculation are well approximated by Eq. (3), we concentrate our analysis on the \hat{T}_2 amplitudes. Examining transferability, we performed a series of NBO CCSD calculations on model saturated hydrocarbons $\text{C}_x\text{H}_{2x+2}$; $x = 3, 4, 5, 6, 7, 8$ and substituted model propanes $\text{C}_3\text{H}_7\text{X}$; $\text{X} = \text{F}, \text{OH}, \text{NH}_2$ using the modest 4-31G basis set. The molecular parameters throughout these model systems were such that (see Figs. 2 and 3, all distances in Å, all angles in degrees): $r_{\text{CH}} = 1.09$, $r_{\text{CC}} = 1.53$, $r_{\text{CN}} = 1.47$, $r_{\text{CO}} = 1.43$, $r_{\text{CF}} = 1.38$, $r_{\text{NH}} = 1.01$, $r_{\text{OH}} = 0.97$, all angles = 109.47° except $\angle\text{HOC} = \angle\text{HNC} = \angle\text{HNH} = 120.0^\circ$, all CH_3 , CH_2 , OH and NH_2 groups staggered with respect to their neighbor

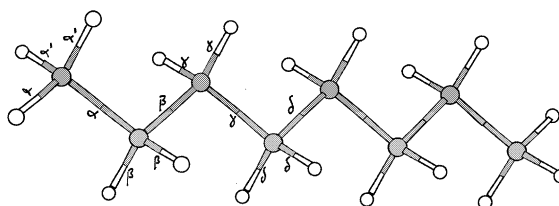


Fig. 2. Location of the type (A), (B), (C) and (D) \hat{T}_2 amplitude excitations within the model saturated hydrocarbon molecules $\text{C}_x\text{H}_{2x+2}$; $x = 3, 4, 5, 6, 7, 8$ corresponding to the data in Table 2.

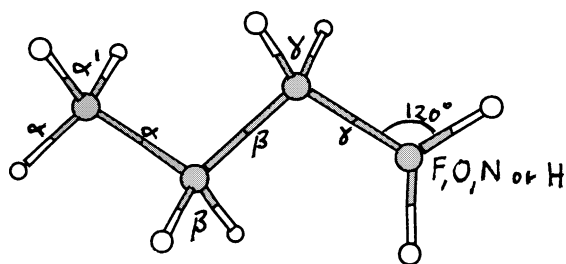


Fig. 3. Location of the type (A), (B), (C) and (D) \hat{T}_2 amplitude excitations within the substituted model propanes C_3H_7X ; $X = F, OH, NH_2, H$ corresponding to the data in Table 3.

groups. The values for the following four types of \hat{T}_2 amplitudes are presented, which also constitute the most important ones for these molecules:

$$\begin{aligned}
 \text{(A)} \quad t_{ii}^{aa}; & \begin{cases} i = \sigma_{CH} \rightarrow a = \sigma_{CH}^* \\ i = \sigma_{XH} \rightarrow a = \sigma_{XH}^* \end{cases} \\
 \text{(B)} \quad t_{ii}^{aa}; & \begin{cases} i = \sigma_{CC} \rightarrow a = \sigma_{CC}^* \\ i = \sigma_{CX} \rightarrow a = \sigma_{CX}^* \end{cases} \\
 \text{(C)} \quad t_{ij}^{ab}; & \begin{cases} i = \sigma_{CC} \rightarrow a = \sigma_{CC}^* \\ j = \sigma_{CC} \rightarrow b = \sigma_{CC}^* \end{cases} \\
 \text{(D)} \quad t_{ij}^{ab}; & \begin{cases} i = \sigma_{CH} \rightarrow a = \sigma_{CH}^* \\ j = \sigma_{CH} \rightarrow b = \sigma_{CH}^* \end{cases}
 \end{aligned} \quad (8)$$

Here σ and σ^* stand for bond and antibond NBOs and excitations are always from the σ, σ^* pair on the same centers. Also i, j (and thus a, b) denote adjacent NBOs having one center in common. Tables 2 and 3 give the results, where the exact location of the corresponding excitation inside the molecule is denoted by greek letters and for clarification was added to Figs. 2 and 3.

Both tables show the great transferability of the selected amplitudes. In the series of paraffins of increasing size (Table 2), the amplitudes on the same location quickly stabilize as the carbon chain length increases. The same type of amplitudes but on different locations inside the molecule also show remarkable equality in their values, also showing signs of stabilization as we move from the end of the molecule to the inside. The results in Table 3 are even more encouraging, since they show a high degree of insensitivity of the amplitudes when introducing different functional groups. As expected the changes are felt most in the immediate vicinity of the new functional group (compare the C_3H_8 and C_3H_7F for example on different locations), especially if the new functional group involves atoms of different electronegativity

Table 2

Type (A), (B), (C) and (D) amplitude values for the \hat{T}_2 amplitudes defined in Eq. (8) for the model saturated hydrocarbon molecules C_xH_{2x+2} ; $x = 3, 4, 5, 6, 7, 8$ in 4-31G basis set

Type	Location	\hat{T}_2 amplitudes					
		C_3H_8	C_4H_{10}	C_5H_{12}	C_6H_{14}	C_7H_{16}	C_8H_{18}
(A)	α	-0.08402	-0.08397	-0.08395	-0.08395	-0.08394	-0.08394
	α'	-0.08373	-0.08371	-0.08370	-0.08370	-0.08369	-0.08369
	β	-0.08395	-0.08358	-0.08356	-0.08355	-0.08355	-0.08355
	γ			-0.08321	-0.08320	-0.08318	-0.08318
	δ					-0.08318	-0.08316
(B)	α	-0.07548	-0.07544	-0.07537	-0.07535	-0.07534	-0.07534
	β		-0.07502	-0.07500	-0.07495	-0.07492	-0.07492
	γ				-0.07500	-0.07493	-0.07491
	δ						-0.07487
(C)	$\alpha\beta$	+0.01875	+0.01885	+0.01886	+0.01886	+0.01886	+0.01886
	$\beta\gamma$			+0.01895	+0.01896	+0.01896	+0.01896
	$\gamma\delta$					+0.01896	+0.01897
(D)	$\alpha\alpha'$	-0.01521	-0.01520	-0.01520	-0.01520	-0.01519	-0.01519
	$\alpha'\alpha'$	-0.01510	-0.01510	-0.01509	-0.01509	-0.01509	-0.01509
	$\beta\beta$	-0.01534	-0.01527	-0.01526	-0.01526	-0.01526	-0.01526
	$\gamma\gamma$			-0.01519	-0.01518	-0.01518	-0.01518
	$\delta\delta$					-0.01518	-0.01518

Table 3

Type (A), (B), (C) and (D) amplitude values for the \hat{T}_2 amplitudes defined in Eq. (8) for the substituted model propanes C_3H_7X ; $X = F, OH, NH_2, H$ in 4-31G basis set

Type	Location	\hat{T}_2 amplitudes			
		C_3H_8	C_3H_7F	C_3H_7OH	$C_3H_7NH_2$
(A)	α	-0.08402	-0.08399	-0.08397	-0.08399
	α'	-0.08373	-0.08367	-0.08369	-0.08371
	β	-0.08395	-0.08387	-0.08397	-0.08369
	γ	-0.08395	-0.08479	-0.08430	-0.08430
	XH			-0.08200	-0.07784
(B)	α	-0.07548	-0.07547	-0.07536	-0.07549
	β	-0.07548	-0.07681	-0.07660	-0.07580
	CX		-0.07583	-0.07658	-0.07485
(C)	$\alpha\beta$	+0.01875	+0.01834	+0.01849	+0.01870
(D)	$\alpha\alpha'$	-0.01521	-0.01510	-0.01513	-0.01517
	$\alpha'\alpha'$	-0.01510	-0.01504	-0.01506	-0.01507
	$\beta\beta$	-0.01534	-0.01535	-0.01540	-0.01524
	$\gamma\gamma$	-0.01534	-0.01648	-0.01591	-0.01560

(H vs. F, O and N). Within the series C_3H_7X ; $X = F, OH, NH_2$ the amplitudes are again remarkably constant, even if the NBO centers involved are similar but different (for example type B) amplitudes on locations α, β and CX). It should however be mentioned that the high transferability found in our example molecules result from the fact that their NBOs are very well localized in space, having NBO occupation numbers >1.95 . Also the distances between the centers are equal or at least very similar, leading to similar hybridization patterns of the underlying NHOs used in the NBO formations in each case.

The \hat{T}_2 amplitude decay as a function of spatial distance between the NBO forming centers can be studied by choosing a larger model paraffin $C_{11}H_{24}$ in the 4-31G basis set. Let us define an average NBO distance \bar{d} between two NBOs as the arithmetic mean between their centers involved:

i th NBO centers	j th NBO centers	\bar{d}_{ij}
p	q	d_{pq}
p	q, r	$(d_{pq} + d_{pr})/2$
p, q	r, s	$(d_{pr} + d_{ps} + d_{qr} + d_{qs})/4$
...

In this table the first entry would correspond, for example, to a pair of core NBOs; the second

entry to a lone-pair/antibond pair; the third to a bond/antibond pair, and so on. Using the average distance we define the total excitation distance D for any \hat{T}_2 amplitude t_{ij}^{ab} as the sum of the average NBO distances corresponding to the individual excitations, $D = \bar{d}_{ia} + \bar{d}_{jb}$. The use of the total excitation distance concept allows us to partition the entire \hat{T}_2 amplitude set into disjoint subsets when partitioning the entire D range into non-overlapping D subranges. Each such amplitude subset is finite in size and thus has at least one amplitude $\max |t_{ij}^{ab}|$, which is larger or equal in magnitude than the others in the same subset. Fig. 4 is a logarithmic plot of $\max |t_{ij}^{ab}|$ vs. the subranges of D defined by their integer parts for the model paraffin $C_{11}H_{24}$. The point at $\text{int}(D)$ gives the largest $|t_{ij}^{ab}|$ value within the \hat{T}_2 amplitude subset defined by all those amplitudes having a D value whose integer part is $\text{int}(D)$.

This plot clearly shows the exponential decay behavior of the entire set of \hat{T}_2 amplitudes. Use of a more diffuse basis set would not change the exponential decay property but it would affect the rate of exponential decay, changing the slope of the array of points in Fig. 4 to a less steep one. A similar exponential decay behavior applies to the antisymmetrized integrals entering the CC correlation energy expression in Eq. (7).

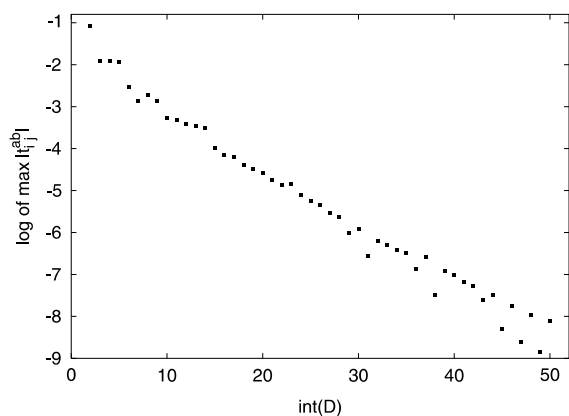


Fig. 4. Plot of $\max |t_{ij}^{ab}|$ vs. $\text{int}(D)$ for the model paraffin $C_{11}H_{24}$. Basis set used was 4-31G.

4. Conclusions

The message of the present investigation is as follows:

I. The \hat{T}_1 amplitudes alone have the power to overcome the minor deficiency of the NBO reference function in describing the HF electron density due to the nature of the NBOs. A set of \hat{T}_1 amplitudes taking the NBO reference function to the HF one is easily found from Thouless theorem via Eq. (3) and their subsequent magnitude changes during a NBO CCSD calculation are comparable to the set of \hat{T}_1 amplitudes obtained from a corresponding HF CCSD calculation.

II. The NBO \hat{T}_2 amplitudes are insensitive to the NBO \rightarrow HF reference correction process, they thus represent the same pairwise electron correlation contribution as for the HF case but in terms of NBOs as basis functions.

III. The NBO \hat{T}_2 amplitudes showed exponential decay behavior as a function of sums of average NBO distances. Hence, the use of a suitably localized set of NBOs as a basis for CC methods seems to be well justified, combining advantages of the MO and AO based schemes, retaining the simplicity of the CC equation formulation in terms of orthogonal MOs, exploiting the potential exponential decay of the CC integrals and amplitudes, and potential transferability. Note also that the use of NBOs easily lend themselves to applying dropped core approximations, the core NBOs

having one very large coefficient on one particular AO and small orthogonality tails on the rest.

Comparing the NBO scheme with the AO based CC methods, in the NBO case we have to screen only \hat{T}_2 amplitudes involving excitations from the occupied to the virtual space, but the AO based CC has to deal with screening the whole $n^2(n^2 + 1)/2$ dimensional AO \hat{T}_2 amplitude set, which includes those representing excitations to the same AOs having considerable long-range character and no exponential but a power decay behavior. All NBO \hat{T}_2 amplitudes t_{ij}^{ab} on the other hand were found to decay exponentially depending on the sum of the average NBO excitation distances $i \leftrightarrow a$ and $j \leftrightarrow b$. Both the NBO and the AO based schemes would have to screen the entire set of integrals for a CCSD calculation.

The observed great transferability of the NBO \hat{T}_2 amplitudes among molecules with similar structures using the same AO basis set, indicates the highly local character of the NBOs. The obvious advantage of amplitude transferability is the possibility to construct correlated wavefunctions for very large systems which would otherwise be impossible to treat directly with present CC programs. The system is partitioned into smaller overlapping subunits, whose size will be governed by the amplitude and integral decay rate, and the local set of relevant amplitudes and integrals determined from a CC calculation on these subunits. The overall CC wavefunction is then simply assembled from the local sets of amplitudes. Note that wavefunction transferability means that not only the energy of the large system becomes accessible but also all other properties. Another obvious use of amplitude transferability would be in creating very good \hat{T}_2 estimates as a starting point for the NBO CC iterations on large systems by simply performing some trivial NBO CC calculations on smaller subunits and transferring the obtained \hat{T}_2 amplitudes.

Finally, we suggest combining very large direct SCF calculations to define \hat{T}_1^0 and introduce the essential electrostatic effects in molecules; then treat correlation by exploiting the transferability of \hat{T}_2 amplitudes. The NBO approach to CC methods offers an interesting and alternative route to exploit the essentially localized treatment of

electron correlation effects in large systems, as an intermediate localized CC approach that fits between the LMO and AO CC formulations.

Acknowledgements

Support by the US National Science Foundation under KDI Award DMR-9980015 is greatly acknowledged.

References

- [1] O. Sinanoğlu, *Adv. Chem. Phys.* 6 (1964) 315.
- [2] R.K. Nesbet, *Adv. Chem. Phys.* 9 (1965) 321.
- [3] M. Häser, J. Almöf, *J. Chem. Phys.* 96 (1992) 489.
- [4] P.E. Maslen, M. Head-Gordon, *Chem. Phys. Lett.* 283 (1998) 102.
- [5] G.E. Scuseria, P.Y. Ayala, *J. Chem. Phys.* 111 (1999) 8330.
- [6] M. Schütz, H.J. Werner, *J. Chem. Phys.* 114 (2001) 661.
- [7] S.F. Boys, *Rev. Mod. Phys.* 32 (1960) 296.
- [8] C. Edmiston, K. Ruedenberg, *Rev. Mod. Phys.* 35 (1963) 457.
- [9] J. Pipek, P.G. Mezey, *J. Chem. Phys.* 90 (1989) 4916.
- [10] S. Saebø, P. Pulay, *Annu. Rev. Phys. Chem.* 44 (1993) 213.
- [11] W.D. Laidig, G.D. Purvis III, R.J. Bartlett, *Int. J. Quantum Chem. Symp.* 6 (1982) 561.
- [12] W.D. Laidig, G.D. Purvis III, R.J. Bartlett, *Chem. Phys. Lett.* 97 (1983) 209.
- [13] W.D. Laidig, G.D. Purvis III, R.J. Bartlett, *J. Phys. Chem.* 89 (1985) 2161.
- [14] A.E. Reed, L.A. Curtiss, F. Weinhold, *Chem. Rev.* 88 (1988) 899.
- [15] F. Weinhold, in: P.v.R. Schleyer, N.L. Allinger, T. Clark, J. Gasteiger, P.A. Kollman, H.F. Schaefer III, P.R. Schreiner (Eds.), *Encyclopedia of Computational Chemistry*, vol. 3, Wiley, Chichester, UK, 1998, pp. 1792–1811.
- [16] A.V. Nemukhin, F. Weinhold, *J. Chem. Phys.* 97 (1992) 1095.
- [17] A.E. Reed, R.B. Weinstock, F. Weinhold, *J. Chem. Phys.* 83 (1985) 735.
- [18] J.P. Foster, F. Weinhold, *J. Am. Chem. Soc.* 102 (1980) 7211.
- [19] D.J. Thouless, *The Quantum Mechanics of Many-Body Systems*, Academic Press, New York, 1961.
- [20] J. Paldus, in: S. Wilson, G.H.F. Dierksen (Eds.), *Methods in Computational Molecular Physics, Series B*, vol. 293, 1991.
- [21] QCPACK, a highly modular *Quantum Chemical PACK*-age written by Norbert Flocke. The package performs standard ab-initio calculations and has SCF, CI and CC capabilities together with NAO and NBO generation programs.
- [22] T.H. Dunning, *J. Chem. Phys.* 53 (1970) 2823.
- [23] J.E. Carpenter, F. Weinhold, *J. Am. Chem. Soc.* 110 (1988) 368.